Proceedings of the 15th Czech and Slovak Conference on Magnetism, Košice, Slovakia, June 17–21 2013

Mössbauer and MFM Investigations of Surface Magnetism in NANOPERM Nanocrystalline Alloys

M. Miglierini[a,b,*], M. Pavúk[a]

[a]Institute of Nuclear and Physical Engineering, Faculty of Electrical Engineering and Information Technology, Slovak University of Technology in Bratislava, Ilkovičova 3, 812 19 Bratislava, Slovakia

[b]Regional Centre of Advanced Technologies and Materials, Palacky University, 17. listopadu 12, 771 46 Olomouc, Czech Republic

Structurally different surface regions are identified at both sides of the ribbon-shaped $^{57}Fe_{90}Zr_7B_3$ NANOPERM alloy. Though paramagnetic in the as-quenched state, the air side shows significant contribution of crystalline bcc-Fe that decreases towards the interior of the ribbon. After annealing at 480 °C, magnetic dipole interactions develop that are associated with enhanced number of ferromagnetic nanograins. Significant increase in the number of nanograins was revealed at the wheel side, while the one at the air side is almost saturated. The observed maze-type magnetic domains exhibit well developed structure with equally wide strips.

DOI: 10.12693/APhysPolA.126.124

PACS: 76.80.+y, 68.37.Rt, 75.60.Ch, 75.70.i, 71.55.Jv

1. Introduction

Nanocrystalline alloys are obtained by controlled annealing from amorphous precursors. The latter are usually prepared in the form of ribbons by rapid quenching on a rotating wheel. This preparation procedure leads to noticeable differences between the bulk and the surfaces of the ribbons. Bulk magnetism is thoroughly studied also by Mössbauer spectrometry [1]. The latter was employed even at elevated temperatures of measurement [2, 3] to follow temperature behaviour of iron nanograins. Their vibrational thermodynamics was recently studied by nuclear inelastic scattering of synchrotron radiation [4].

Nevertheless, little is known about structural deviations that are observed at the opposite sides of the ribbons. In the present work, the impact of structural differences on the resulting surface magnetism is investigated in the well-known $Fe_{90}Zr_7B_3$ NANOPERM alloy in as-quenched and annealed states, using surface sensitive analytical techniques.

Magnetic domain structure reflects the behaviour of magnetization. In a nanocrystalline material, its character is determined largely by residual anisotropies [5, 6], since the size of domains extends over a large number of grains. As the method for obtaining the image of a domain structure we used the magnetic force microscopy (MFM), which is so far rarely used in the study of nanocrystalline materials [7, 8].

2. Experimental details

Conversion Electron (CEMS) and Conversion X-ray (CXMS) Mössbauer Spectroscopy that scan the surface regions down to the depth of about 200 nm and 1000 nm, respectively were used with a $^{57}Co/Rh$ radioactive source. To enhance their diagnostic potential we have used samples enriched to 63% with the isotope ^{57}Fe. As-quenched and annealed (for 10 min at 480 °C) alloys were inspected. The topography of the surface and magnetic force gradients in its vicinity were obtained at room temperature by Dimension Edge atomic force microscope (Veeco, USA).

3. Results and discussion

In the as-quenched state, the $^{57}Fe_{90}Zr_7B_3$ alloy is mostly paramagnetic. This is demonstrated by a pronounced central Mössbauer broadened signal (light grey spectral component) at the wheel side (Fig. 1a), while only traces of this doublet can be seen at the air side (Fig. 1b). The air side of the ribbon was exposed to the surrounding atmosphere during the production process. A noticeable surface crystallization is observed namely at this side. The six-line dark grey patterns correspond to bcc-Fe nanograins.

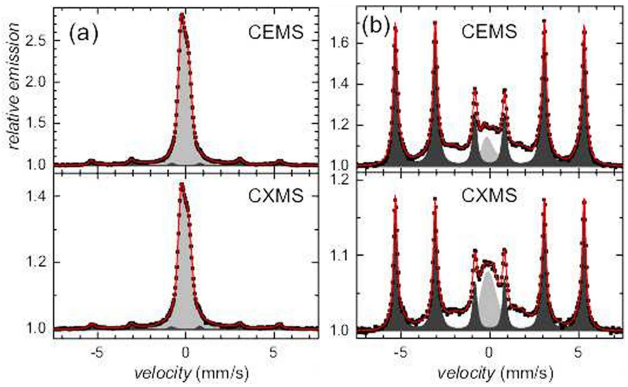

Fig. 1. CEMS and CXMS spectra of the as-quenched $^{57}Fe_{90}Zr_7B_3$ alloy recorded at the wheel (a) and air (b) side.

*corresponding author; e-mail: marcel.miglierini@stuba.sk

After annealing, the quantity of bcc-Fe nanograins has significantly increased namely at the wheel side. Their amount at the air side seems to be almost saturated with only minor development, as seen from Fig. 2 and Table.

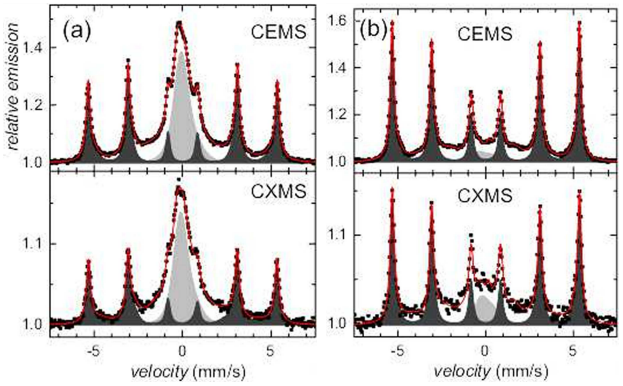

Fig. 2. CEMS and CXMS spectra of the annealed $^{57}Fe_{90}Zr_7B_3$ alloy recorded from the wheel (a) and air (b) side.

TABLE

Total amount of the crystalline phase, A_r (%) and average magnetic hyperfine field of the amorphous residual phase, B_{hf} (T) in the $^{57}Fe_{90}Zr_7B_3$ as derived from Mössbauer spectrometry (error margins are ±1.5% and ±0.1 T, respectively).

sample	wheel side					air side			
	CEMS		CXMS			CEMS		CXMS	
	A_r	B_{hf}	A_r	B_{hf}		A_r	B_{hf}	A_r	B_{hf}
as-quenched	11	3.8	12	3.8		69	16.3	59	17.2
annealed	43	14.7	41	11.6		74	17.5	63	18.3

At the air side of the as-quenched ribbon, the bcc-Fe nanograins are predominantly located in the near-surface regions (<200 nm). Their number decreases by ca. 10% towards the interior. Exchange interactions among the grains polarize the amorphous matrix. This gives rise to hyperfine magnetic fields that are higher in deeper subsurface regions (Table). A homogeneous distribution of bcc-Fe is found at the wheel side irrespective of the depth. Their amount is too low for establishing a magnetic order. In the annealed samples, the crystallization has developed more rapidly at the wheel side compared to the air one. The hyperfine magnetic fields depend upon the amount of nanograins.

MFM phase-domain sensitive images exhibit very tiny (note the scanned area) strips (Fig. 3a) with rather chaotic arrangement at the air side (Fig. 3b) of the as-quenched alloy. This side of the ribbon displays after annealing a well distinguished magnetic order (Fig. 3d). The observed strips are uniformly wide with a periodicity of about 0.9 μm. Much bigger domains were found at the wheel side (Fig. 3c).

4. Conclusions

Using the techniques that are sensitive to surface features of structural, as well as magnetic, origin to diverse

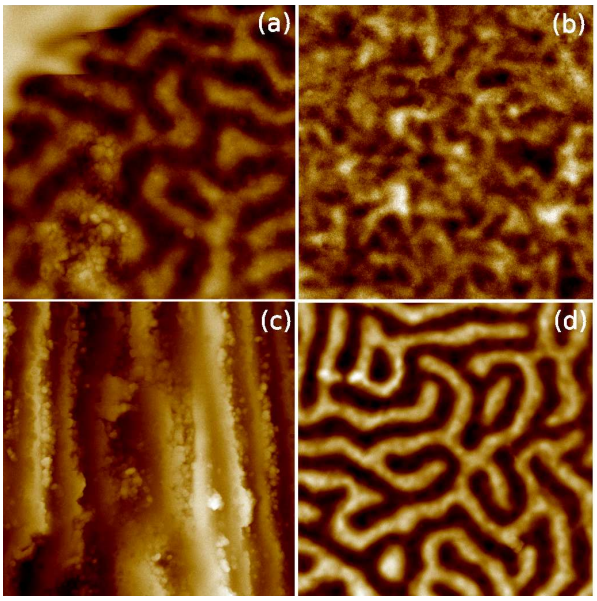

Fig. 3. MFM images of the as-quenched 5×5 μm^2 (a, b) and annealed 10×10 μm^2 (c, d) $^{57}Fe_{90}Zr_7B_3$ alloy recorded at the wheel (a, c) and air (b, d) sides of the ribbon.

depths, viz. CEMS and CXMS, we were able to differentiate among contributions from structurally different regions in the $^{57}Fe_{90}Zr_7B_3$ NANOPERM alloy that have developed at the wheel and air sides of the ribbons. Magnetic dipole interactions give a picture of magnetic states via phase-domain MFM images.

Acknowledgments

This work was supported by the research projects VEGA 1/0286/12, SK-PL-0032-12, CZ.1.05/2.1.00/03.0058, and CZ.1.07/2.3.00/20.0155.

References

[1] I. Škorvánek, M. Miglierini, P. Duhaj, *Mater. Sci. Forum* **235-238**, 771 (1997).

[2] S. Stankov, B. Sepiol, T. Kaňuch, D. Scherjau, R. Würschum, M. Miglierini, *J. Phys.: Condens. Matter.* **17**, 3183 (2005).

[3] M. Miglierini, J.-M. Grenèche, *J. Phys.: Condens. Matter.* **15**, 5637 (2003).

[4] S. Stankov, M. Miglierini, A.I. Chumakov, I. Sergueev, Y.Z. Yue, B. Sepiol, P. Svec, L. Hu, R. Rüffer, *Phys. Rev. B* **82**, 144301 (2010).

[5] O. Životský, K. Postava, L. Kraus, K. Hrabovská, A. Hendrych, J. Pištora, *J. Magn. Magn. Mater.* **322**, 1523 (2010).

[6] J.M. Silveyra, G. Vlasák, P. Švec, D. Janičkovič, V.J. Cremaschi, *J. Magn. Magn. Mater.* **322**, 2797 (2010).

[7] I. García, N. Iturriza, J.J. del Val, H. Grande, J.A. Pomposo, J. González, *J. Magn. Magn. Mater.* **322**, 1822 (2010).

[8] X. Bao, X. Gao, J. Zhu, S. Zhou, *J. Rare Earths* **29**, 939 (2011).